

# The Whittle likelihood for mixed models with application to groundwater level time series

Jakub J. Pypkowski<sup>1,\*</sup>, Adam M. Sykulski<sup>1</sup>, James S. Martin<sup>1</sup>, Ben P. Marchant<sup>2</sup>

1 December 2025

## Abstract

Understanding the processes that influence groundwater levels is crucial for forecasting and responding to hazards such as groundwater droughts. Mixed models, which combine a fixed mean, expressed using independent predictors, with autocorrelated random errors, are used for inference, forecasting and filling in missing values in groundwater level time series. Estimating parameters of mixed models using maximum likelihood has high computational complexity. For large datasets, this leads to restrictive simplifying assumptions such as fixing certain free parameters in practical implementations. In this paper, we propose a method to jointly estimate all parameters of mixed models using the Whittle likelihood, a frequency-domain quasi-likelihood. Our method is robust to missing and non-Gaussian data and can handle much larger data sizes. We demonstrate the utility of our method both in a simulation study and with real-world data, comparing against maximum likelihood and an alternative two-stage approach that estimates fixed and random effect parameters separately.

**Keywords:** Drought, Matérn covariance, missing values, precipitation, predictors, regression

## 1 Introduction

Groundwater levels (GWLS) are recorded by measuring the water level in observation boreholes. A time series of GWL measurements from one borehole, called a groundwater hydrograph, reflects changes in the amount of water stored in a water-bearing layer of rock material called an aquifer. In particular, hydrographs can be used to detect and study groundwater droughts, a natural hazard defined as a period of substantially reduced availability of groundwater. Groundwater droughts may lead to costly

---

<sup>1</sup> Imperial College London, Department of Mathematics, London, SW7 2AZ, United Kingdom

<sup>2</sup> British Geological Survey, Keyworth, NG12 5GG, Nottingham, United Kingdom

\* Corresponding author; email: jakub.pypkowski22@imperial.ac.uk

restrictions of water supply for households, agriculture, and industry, as well as cause environmental damage [Marchant and Bloomfield, 2018, and references therein]. A successful response to groundwater droughts requires reliable forecasting, accurate warning systems, and sound water management plans [van Lanen et al., 2016]. These require a good understanding of the processes driving droughts and necessitates models for GWLs.

Various assessment tools require that GWL data are collected at regular time steps and are complete [see e.g. Bloomfield and Marchant, 2013, ElHaj and Alshamsi, 2025]. In reality, such standards are rarely achieved, and missing values must be filled in [Marchant and Bloomfield, 2018, Vu et al., 2021]. Approaches to this vary from simple heuristics such as adopting a local mean, median, or linear interpolation between nearest observed values [ElHaj and Alshamsi, 2025, Peterson and Western, 2018], to complex, physics-based flow models [e.g. Mackay et al., 2014, Zhou and Li, 2011], which can also be used for inference and forecasting. The former approaches may not be scientifically justified in certain cases, while the latter models may be too complex to estimate when there are insufficient data, particularly when some predictor information is missing [Marchant et al., 2022]. Recent developments in neural networks gave rise to Long Short-Term Memory models, which can fill in missing GWL values using few inputs, but do not provide insights into processes driving changes to GWLs [e.g. Gholizadeh et al., 2023, Vu et al., 2021].

To bridge this gap, statistical modelling can be used. Peterson and Western [2018] proposed a method which consists in estimating a nonlinear transfer function noise model [TFN, Peterson and Western, 2014], fitting an exponential covariance model to the variogram of the residuals, and using Kriging to interpolate. The TFN approach combines two ways of modelling GWLs: using independent meteorological variables, precipitation and potential evapotranspiration, as predictors, and modelling infiltration dynamics through a soil-moisture partitioning model [for details see Peterson and Western, 2014]. Obtaining estimates of the model parameters involves solving an ordinary differential equation, and optimising an objective function given as a transformed sum of weighted squared innovations [von Asmuth and Bierkens, 2005].

An alternative approach using a mixed model was developed by Marchant and Bloomfield [2018] and Marchant et al. [2022]. They modelled GWLs as a sum of a fixed term and an autocorrelated random term and, similarly to Peterson and Western [2018], used Kriging to fill in missing values. The fixed term was expressed as a function of independent predictors including trends, seasonality, and meteorological variables (via impulse response functions), and then combined with random errors generated by a Gaussian process with an exponential covariance function. The model parameters were estimated using the Gaussian maximum likelihood. Both components of the model, fixed and random, were fitted simultaneously, unlike in Peterson and Western [2018], who estimated the fixed and random effects parameters in successive steps. The mixed model approach requires relatively few inputs and is

simpler than physics-based models. Marchant and Bloomfield [2018] used the mixed model to group hydrographs across two aquifers in the UK by the main factors driving their variability and Marchant et al. [2022] confirmed that the mixed model performs well at filling in missing values. Because the mixed model incorporates a model for random errors, it allows for quantifying uncertainty. Through this, Marchant et al. [2022] also used it to detect outliers, and Marchant and Bloomfield [2018] proposed that it can be used for forecasting the risk of droughts.

There are two limitations in these state-of-the-art GWL models we seek to address in this paper. The first is the assumption of Gaussian errors, where models with a more general distribution of the error term may provide a better fit to GWL data [Marchant et al., 2016]. The second is the computational cost of maximum likelihood estimation, which increases steeply with the time series length  $n$ . This is due to the covariance matrix inversion in the Gaussian likelihood, which is  $O(n^3)$  in general, with modern algorithms reducing it to approx.  $O(n^{2.37})$  [see e.g Alman and Williams, 2024]. In the idealised case of a complete, regularly-sampled, and stationary time series, the covariance matrix becomes a Toeplitz matrix, inverting which has computational complexity of  $O(n^2)$  [Trench, 1964]. In practice, data are available at weekly, daily, or even 15-minute intervals and go as far back as the mid-19th century [Marchant and Bloomfield, 2018]. Maximum likelihood can therefore only be run on sub-sampled segments of such datasets.

To overcome these limitations, we propose a likelihood approximation method drawing from the Whittle likelihood [Whittle, 1953]. The Whittle likelihood has become a common tool in estimating parameters of covariance models in second-order stationary time series. In this paper, we propose a Whittle-based method which simultaneously estimates all parameters of mixed models, can incorporate flexible forms of nonlinear means with impulse response functions, and can handle time series with missing data, all of which are important for GWL time series modelling and estimation in practice. This is done by integrating existing Whittle methods for regression-based models with recent developments for Whittle inference of stationary time series with missing data. Like the standard Whittle likelihood for stationary time series, our method does not require that random errors are Gaussian, only that they are fourth-order stationary. Similarly, our method retains the order  $O(n \log n)$  of computational complexity of the standard Whittle likelihood. In a simulation study, we verify that our method can be successfully applied to data that exhibit characteristics typical for GWL measurements, including large volumes of missing data and non-Gaussianity.

Several Whittle likelihood adaptations have been proposed for nonstationary processes [e.g. Dahlhaus, 2000, Li et al., 2021, Rosen et al., 2012], but these works are focussed on capturing nonstationarity in the covariance of the error term, for instance through local stationarity. They do not, however, consider a fixed nonstationary mean using independent variables. To this end, Ivanov and Prykhod'ko [2016] and Ivanov et al. [2020] proposed a two-step procedure for models with a nonstationary mean driven

by independent variables combined with Gaussian or Lévy noise, respectively. In the first step of the procedure, the mean was estimated using least squares, and in the second step the Whittle likelihood was applied to the residuals. The advantage of our approach is that it simultaneously estimates the parameters of the fixed mean and the covariance of the error term, leading to reduced estimation error, as we shall show through a simulation study. Simultaneous estimation of all parameters using Whittle-based methods has been explored in several scenarios. Bertolacci et al. [2022] used it for models with an unknown fixed non-zero mean. Koul and Surgailis [2008] proposed a method for long-memory moving average processes, and Wang and Xia [2015] and Huang et al. [2016] proposed a method for ARMA-type models, which was further adapted by Wei et al. [2022] and Baltagi et al. [2025] to estimation in panel data. Goodwin et al. [2025] proposed a Bayesian inference method for models with long-range dependence of the error term. In all these approaches, the unobserved error term is modelled by subtracting the unknown mean, expressed as a function of free parameters, from the observed data. Such subtraction of the mean function is the key component of our framework, which we extend in this paper to handle time series with missing data as well as nonlinearity in the mean through impulse response functions.

Our method directly responds to challenges presented by GWL modelling, but its applicability extends beyond this area. First, filling in missing values is a common challenge in areas such as meteorology [e.g. Coutinho et al., 2023 Rahman et al., 2024, Shabalala et al., 2019], or for other types of time series data in hydrology, such as streamflow [Hiben et al., 2024], soil moisture [Myeni et al., 2022], and water quality monitoring [Zhang and Thorburn, 2022]. Second, the method can be used with any time series where one is interested in modelling the mean, typically through regression, with autocorrelated error terms. Such problems are encountered in various areas of science, examples of which include pollution modelling [Yu et al., 2017] and astrostatistics [Aigrain and Foreman-Mackey, 2023].

The rest of this paper is structured as follows. We introduce the GWL data and present details of the mixed model in Section 2. In Section 3, we formulate our framework for parameter estimation of a mixed model using the Whittle likelihood. We also outline two alternative estimation methods: Gaussian maximum likelihood and two-stage Whittle estimation. We perform a simulation study in Section 4, in which we assess the performance of the presented estimation methods in various scenarios, which focus on challenges typical to GWL modelling including missing data and non-Gaussian observations. In Section 5, we model real-world GWL data using our Whittle-based framework. Lastly, we present our concluding remarks in Section 6.

## 2 Data and the mixed model

### 2.1 Data

We consider monthly GWL time series obtained from six observation boreholes across Southern England, which we identify with letters A–F. The time series span a period of 720 months from January 1960 to December 2019, and were obtained under the Open Government Licence v3.0 from the Environment Agency’s Hydrology Data Explorer (<https://environment.data.gov.uk/hydrology/landing>). Figures 1–2 illustrate locations of the boreholes and corresponding time series, respectively. All time series exhibit yearly seasonality, which in the case of boreholes B and C dominates the overall variability of GWLs. In combination with longer-term trends (over a decade), seasonality is also a strong feature of the GWLs in borehole A. In boreholes D–F, seasonality gives way to medium-term features (up to 10 years). These patterns of variation within the hydrographs are broadly consistent with those observed by Marchant and Bloomfield [2018], who performed a cluster analysis of standardised hydrographs in and around the Chalk aquifer. The Chalk aquifer is the major aquifer of southern and eastern England and includes the majority of the highly productive aquifers shown in Figure 1. One cluster contained boreholes from the Chilterns (in the vicinity of borehole E) and the eastern end of the North Downs (boreholes D and F). Consistent with Figure 2, this cluster was characterised by relatively smooth hydrographs caused by deposits overlying the Chalk, which result in significant groundwater storage or delays to recharge. The cluster covering the South Downs (borehole B) was characterised by relatively rough hydrographs reflecting the highly fractured and faulted nature of this part of the aquifer. Borehole

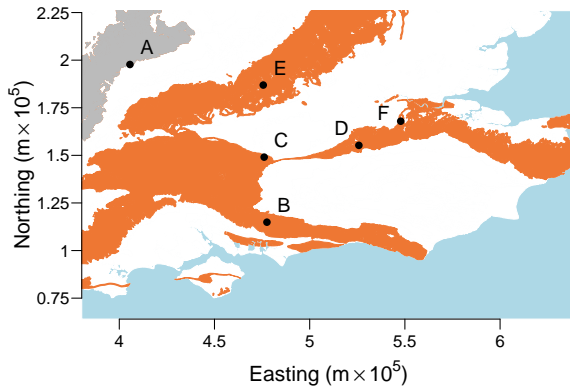


Figure 1: Locations of observation boreholes A–F across Southern England. Coloured areas show highly productive aquifers in which flow is virtually all through fractures and other discontinuities as per British Geological Survey 625K digital hydrogeological map (<https://www.bgs.ac.uk/datasets/hydrogeology-625k/>). Great Oolite and Inferior Oolite groups are shown in grey. Other aquifers, the vast majority of which are part of the Chalk aquifer, are shown in orange. Contains British Geological Survey materials © UKRI 2025. Contains OS data © Crown copyright and database rights 2025. Contains public sector information licensed under the Open Government Licence v3.0.

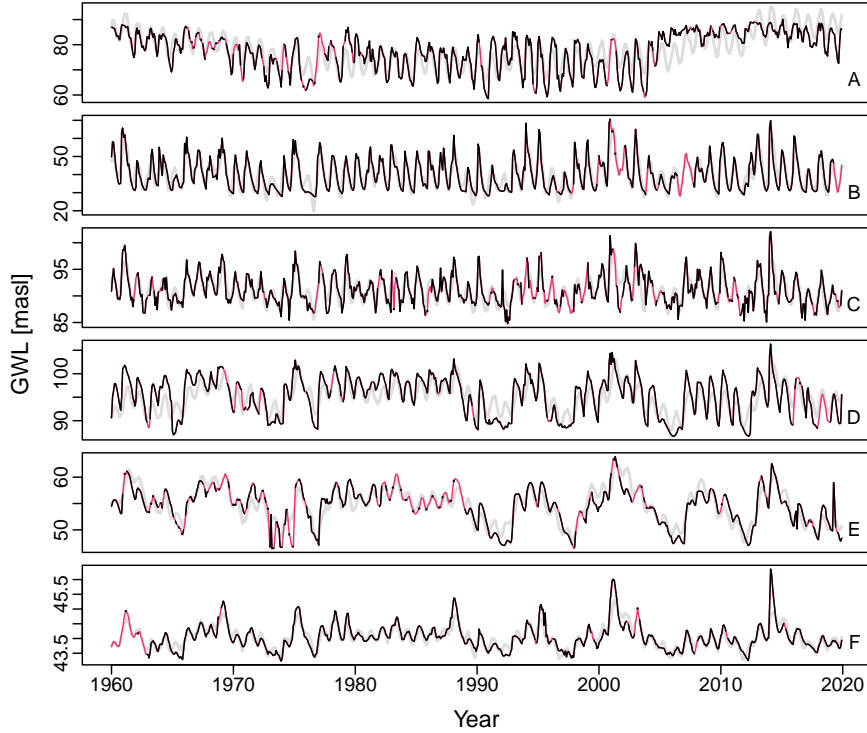


Figure 2: Recorded groundwater levels (black), missing value predictions (magenta) and estimated fixed-term mean (grey) for boreholes A–F (magenta and grey lines obtained using our Whittle-based method of Section 3). Black lines represent periods of no missing records, and black dots represent isolated observations. Contains data from the Environment Agency’s Hydrology Data Explorer © Crown copyright 2025. Contains public sector information licensed under the Open Government Licence v3.0.

C, at the western end of the North Downs, corresponds to a cluster characterised by hydrographs with moderate smoothness. Borehole A lies in the Great Oolite aquifer, a Jurassic limestone aquifer. This aquifer is characterised by a combination of low storage ability (storativity) and high ability to transfer water (transmissivity) [Neumann et al., 2003]. This makes GWLs in this aquifer highly responsive to meteorological factors and leads to large seasonal variation.

The six time series are characterised by different missingness patterns. The fractions of data missing vary from 4.9% for borehole D to 22.1% for borehole E. The longest consecutive period of missing observations is 15 months, which occurred in years 2006–2007 in borehole B. On the other extreme, there are 126 instances of records missing for only one month across the six time series.

To model GWLs, we use monthly rainfall data from Tanguy et al. [2021] for locations of boreholes A–F from February 1950 to December 2019. We deseasonalise the rainfall data by removing a corresponding month’s mean (across all years) from each observation.

## 2.2 Mixed model

In this paper, we focus on the estimation of the mixed model developed by Marchant and Bloomfield [2018] and Marchant et al. [2022]. In this approach, the mean of the process driving the GWL variation is assumed to be a linear model of terms including trend, seasonality, and a response to meteorological variables. We call these components of the model describing the mean collectively as the *fixed* term. The *random* term describes the marginal distribution and covariance structure of the random error. GWL, the response variable, is modelled as a sum of fixed and random terms. The model for each borehole can therefore be written as

$$\mathbf{x} = M_{\gamma}\boldsymbol{\beta} + \boldsymbol{\epsilon}, \quad (1)$$

where  $\mathbf{x} = (x_1, \dots, x_n)^T$  is a vector of  $n$  GWL measurements,  $M_{\gamma}$  is an  $n \times m$  design matrix containing  $n$  values of  $m$  covariates,  $\boldsymbol{\beta}$  is a vector of  $m$  regression parameters, and  $\boldsymbol{\epsilon}$  is a vector of  $n$  random errors.

The fixed term is linear in  $\boldsymbol{\beta}$ , however some columns of the design matrix  $M_{\gamma}$  depend on the parameter vector  $\gamma$  through an impulse response function (IRF), as we shall explain later in this section. This introduces nonlinearity to the mixed model. The autocorrelation of the random error  $\boldsymbol{\epsilon}$  is controlled by the parameter vector  $\alpha$ . We first present the construction of the fixed term which involves the following covariates:

1. An **intercept** encoded by a column of 1's in the design matrix  $M_{\gamma}$ .
2. A long-term **linear trend** encoded in  $M_{\gamma}$  as  $(1/n, 2/n, \dots, 1)^T$ .
3. **Seasonal variation** encoded by two columns of  $M_{\gamma}$ : one containing entries given by  $\sin(2\pi t/12)$  and the other by  $\cos(2\pi t/12)$ , where  $t$  is time (in months).
4. **Temporary trends** encoded by several columns of  $M_{\gamma}$ , each containing a cyclic spline basis function [Wood, 2017, p.202–204]. Each basis function covers a different period and captures a deviation from the linear trend during a given period. Knots of the basis functions are spaced evenly. When the basis functions are used, the intercept becomes redundant and is excluded from the model.
5. **Response to precipitation** encoded through an impulse response function [IRF, von Asmuth et al., 2002]. By using the IRFs, we account for a lagged response to precipitation, which is expected in GWLs. At the same time, we keep the number of model parameters low relative to an approach where one directly includes precipitation at multiple lags in the design matrix. IRFs aggregate the precipitation data, while assigning weights to precipitation at different lags. The weights reflect the importance of precipitation at a given lag for the GWL. The corresponding column  $(m_1, \dots, m_n)^T$  of  $M$  is given by

$$m_t = \sum_{\tau=0}^{n_{IRF}-1} \text{IRF}(\tau)p(t-\tau), \quad (2)$$

where  $n_{IRF} - 1$  is the maximum lag considered, and  $p(t - \tau)$  is precipitation at time  $t - \tau$ . The weights assigned to an observation at lag  $\tau$  are equal to the value of the chosen IRF function given by

$$IRF(\tau; A, s, a) = A \frac{a^s (\tau + 1)^{s-1} \exp[-a(\tau + 1)]}{\Gamma(s)}. \quad (3)$$

Marchant et al. [2022] normalised the IRFs, by fixing  $A$  so that the sum  $\sum_{\tau=0}^{n_{IRF}-1} IRF(\tau; A, a, s) = 1$ . We follow the same approach and as a result rewrite the entries  $m_t$  given in (2) as

$$m(t; s, a) = \frac{\sum_{\tau=0}^{n_{IRF}-1} (\tau + 1)^{s-1} \exp[-a(\tau + 1)] p(t - \tau)}{\sum_{\kappa=0}^{n_{IRF}-1} (\kappa + 1)^{s-1} \exp[-a(\kappa + 1)]}. \quad (4)$$

The GWL depends on precipitation nonlinearily through the parameters  $\gamma = (s, a)^T$ . We set  $n_{IRF} = 120$ .

We model the error term  $\epsilon = (\epsilon_1, \dots, \epsilon_n)^T$  as a realisation of a zero-mean continuous time process  $\epsilon(t; \alpha)$  at integer times  $(\epsilon(1, \alpha), \dots, \epsilon(n, \alpha))$ . We denote the covariance of errors  $\epsilon_t, \epsilon_{t+\tau}$ , for any  $t$ , as  $c_\alpha(\tau) = c_\alpha(\epsilon_t, \epsilon_{t+\tau})$ . We consider a nested-nugget Matérn covariance given as

$$c_\alpha(\tau) = \begin{cases} c_0 + c_1 & \text{if } \tau = 0, \\ \frac{c_1}{2^{\nu-1} \Gamma(\nu)} \left( \frac{2\sqrt{\nu}\tau}{\lambda_m} \right)^\nu K_\nu \left( \frac{2\sqrt{\nu}\tau}{\lambda_m} \right) & \text{if } \tau > 0, \end{cases} \quad (5)$$

where  $K_\nu(\cdot)$  is the modified Bessel function of the second kind of order  $\nu$ , and  $\alpha = (c_0, c_1, \lambda_m, \nu)^T$  is a vector of parameters called: nugget, partial sill variance, length-scale, and smoothness, respectively. For some boreholes, we further consider a covariance function given as a product of Matérn and periodic covariance functions (which we shall refer to as Matérn-periodic), that is (5) multiplied by a periodic kernel  $\exp(-2\sin(\pi\tau/p)/\lambda_p^2)$  if  $\tau > 0$ , where  $p$  is the period and  $\lambda_p$  is the length-scale of the periodic kernel. This allows for random periodic effects to be captured if present in the data.

Marchant and Bloomfield [2018] and Marchant et al. [2022] assumed that  $\epsilon(t, \alpha)$  is a Gaussian process in order to perform Gaussian maximum likelihood estimation. Our Whittle likelihood for mixed models (see Section 3.1) allows us to relax this assumption: we do not specify a marginal distribution of the random term, instead we only require that it is fourth-order stationary. Marchant and Bloomfield [2018] and Marchant et al. [2022] pre-set the smoothness parameter of the Matérn covariance to  $\nu = 1/2$  to reduce the number of parameters and speed up computation. This yields a simpler, exponential covariance, where  $c_\alpha(\tau) = c_1 \exp(-\tau/\lambda_m)$  if  $\tau > 0$ . In this paper, we shall use our new methodology to estimate all four parameters of the Matérn covariance, and for borehole A we shall estimate five parameters of the Matérn-periodic covariance with a fixed period.

### 3 The Whittle likelihood for mixed models

In this section, we formulate our frequency-domain framework for estimating parameters of the mixed model. We first introduce the standard Whittle likelihood for second-order stationary processes [Whittle, 1953], which is commonly used for the estimation of covariance parameters of random processes with zero mean. We then introduce adaptations that allow for the estimation of parameters of the fixed term of the mixed model. We integrate two recent developments in the Whittle literature into our framework: modulation [Guillaumin et al., 2017], which allows for estimation in datasets with missing values, and debiasing [Sykulski et al., 2019], which improves accuracy of the estimation. Following the introduction of our method in Section 3.1, we present two alternative estimation methods in Section 3.2, including the Gaussian maximum likelihood. Once the parameters of the mixed model are estimated, they can be used for inference, filling in missing values, and forecasting. We perform the latter two using the simple Kriging predictor, for which we treat the estimated fixed term as a known mean [see van Lieshout, 2019, p.26–27 for details].

#### 3.1 Method formulation

Let  $Y(t; \boldsymbol{\alpha})$  be a zero-mean continuous-time Gaussian process with stationary covariance given by some covariance function  $c_{\boldsymbol{\alpha}}(\tau)$ , and let  $\mathbf{y} = (y(1, \boldsymbol{\alpha}), \dots, y(n, \boldsymbol{\alpha})) = (y_1, \dots, y_n)$  be a finite, discrete-time realisation of the process at integer times. The spectral density function (sdf) of  $Y(t; \boldsymbol{\alpha})$  for frequency  $\omega_j$ , when it exists, is given by

$$f_{\boldsymbol{\alpha}}(\omega_j) = \int_{-\infty}^{\infty} c_{\boldsymbol{\alpha}}(\tau) \exp(-i\omega_j \tau) d\tau. \quad (6)$$

The periodogram, an estimate of the sdf obtained using  $\mathbf{y}$ , is

$$I_j = \frac{1}{n} \left| \sum_{t=1}^n y_t \exp(-i\omega_j t) \right|^2, \quad (7)$$

where  $\omega_j \in \frac{2\pi}{n}(-\lceil n/2 \rceil + 1, \dots, -1, 0, 1, \dots, \lfloor n/2 \rfloor)$ . The log-likelihood for a Gaussian process can be written as

$$l(\boldsymbol{\alpha}) = \text{constant} - \frac{1}{2} \log|C(\boldsymbol{\alpha})| - \frac{1}{2} \mathbf{y}^T C(\boldsymbol{\alpha})^{-1} \mathbf{y}, \quad (8)$$

where  $C(\boldsymbol{\alpha})$  is the covariance matrix of the discrete-time realisation  $\mathbf{y}$ . The Whittle likelihood [Whittle, 1953] approximates the log-likelihood in the frequency domain up to fixed constants, and is given in its discretised form by

$$l_W(\boldsymbol{\alpha}) = - \sum_{j=1}^n \left[ \log f_{\boldsymbol{\alpha}}(\omega_j) + \frac{I_j}{f_{\boldsymbol{\alpha}}(\omega_j)} \right]. \quad (9)$$

An argument  $\hat{\boldsymbol{\alpha}}$  which maximises  $l_W(\boldsymbol{\alpha})$  is called a Whittle estimate. The computation of the Whittle likelihood is of order  $O(n \log n)$  using the Fast Fourier Transform (FFT), which is lower than the computation of the Gaussian log-likelihood of (8), which requires matrix inversion. Another useful feature

of the Whittle likelihood is that it is often robust to non-Gaussianity as the parameter estimates are consistent and asymptotically normal for all fourth-order stationary processes, as long as fourth-order moments are finite and fourth-order cumulants are absolutely summable [Dahlhaus, 1988, Guillaumin et al., 2022, Sykulski et al., 2019]. This encompasses many stochastic processes that are not Gaussian.

We propose the following modification of the Whittle likelihood to adapt it for parameter estimation in a mixed model. Since the unobserved mixed model error process  $\epsilon(t; \boldsymbol{\alpha})$  satisfies the conditions imposed on  $Y(t; \alpha)$ , we compute the periodogram of  $\epsilon(t; \boldsymbol{\alpha})$  from the mixed model residuals  $\mathbf{x} - M_{\boldsymbol{\gamma}}\boldsymbol{\beta}$ . The periodogram is therefore a function of the unknown  $\boldsymbol{\beta}$  and  $\boldsymbol{\gamma}$  given as

$$I_j(\boldsymbol{\beta}, \boldsymbol{\gamma}) = \frac{1}{n} \left| \sum_{t=1}^n \left[ x_t - M_{\boldsymbol{\gamma}}^{(t)} \boldsymbol{\beta} \right] \exp(-i\omega_j t) \right|^2, \quad (10)$$

where  $M_{\boldsymbol{\gamma}}^{(t)}$  denotes the  $t$ -th row of the design matrix. We replace  $I_j$  in (9) by  $I_j(\boldsymbol{\beta}, \boldsymbol{\gamma})$ , and yield the Whittle likelihood expressed jointly as a function of  $\boldsymbol{\alpha}$ ,  $\boldsymbol{\beta}$ , and  $\boldsymbol{\gamma}$ :

$$l_W(\boldsymbol{\alpha}, \boldsymbol{\beta}, \boldsymbol{\gamma}) = - \sum_{j=1}^n \left[ \log f_{\boldsymbol{\alpha}}(\omega_j) + \frac{I_j(\boldsymbol{\beta}, \boldsymbol{\gamma})}{f_{\boldsymbol{\alpha}}(\omega_j)} \right]. \quad (11)$$

We call arguments  $\hat{\boldsymbol{\alpha}}$ ,  $\hat{\boldsymbol{\beta}}$ ,  $\hat{\boldsymbol{\gamma}}$  which maximise  $l_W(\boldsymbol{\alpha}, \boldsymbol{\beta}, \boldsymbol{\gamma})$  Whittle estimates of  $\boldsymbol{\alpha}$ ,  $\boldsymbol{\beta}$ , and  $\boldsymbol{\gamma}$ .

In addition to being computationally efficient through the use of the FFT, the Whittle likelihood has desirable asymptotic properties for fourth-order stationary residuals. In finite samples, however, it may exhibit poor performance, in particular leading to a large estimation bias [see e.g. Dahlhaus, 1988, Sykulski et al., 2019]. This results from spectral blurring, an issue common in spectral analysis [Percival and Walden, 1993], caused by the truncation of stochastic processes to finite-length samples. Sykulski et al. [2019] proposed a modification of the Whittle likelihood called debiasing, and showed that it can substantially reduce bias in finite samples. It consists in replacing the sdf in (9) with the expected periodogram given by

$$\bar{f}_{\boldsymbol{\alpha}}(\omega_j) = \mathbb{E}(I_j) = 2\text{Re} \left[ \sum_{\tau=0}^{n-1} \left( 1 - \frac{\tau}{n} \right) c_{\boldsymbol{\alpha}}(\tau) \exp(-i\omega_j \tau) \right] - c_{\boldsymbol{\alpha}}(0), \quad (12)$$

which can be computed via an FFT. We apply the same modification to the proposed Whittle likelihood for mixed models in (11).

To be fit for our purpose, the Whittle likelihood must also allow for missingness in the data. To ensure this, we further refine our method by combining it with a framework proposed by Guillaumin et al. [2017] on modulated time series. Let  $\mathbf{g} = (g_1, \dots, g_n)$  be a modulating sequence such that

$$g_t = \begin{cases} 1 & \text{if the value of } x_t \text{ is observed,} \\ 0 & \text{otherwise.} \end{cases} \quad (13)$$

Then the modulated time series is given as  $\tilde{\mathbf{x}} = (\tilde{x}_1, \dots, \tilde{x}_n) = (x_1 g_1, \dots, x_n g_n)$ , meaning it takes the value of  $x_t$  if it is observed, or 0 if it is not. Analogous to Guillaumin et al. [2017], we introduce the following modifications to our Whittle likelihood for mixed models. We first replace the periodogram of residuals with a periodogram of modulated residuals

$$\tilde{I}_j(\boldsymbol{\beta}, \boldsymbol{\gamma}) = \frac{1}{n} \left| \sum_{t=1}^n g_t \left[ x_t - M_{\boldsymbol{\gamma}}^{(t)} \boldsymbol{\beta} \right] \exp(-i\omega_j t) \right|^2, \quad (14)$$

and then obtain its expectation as

$$\tilde{f}_{\boldsymbol{\alpha}}(\omega_j) = \mathbb{E}[\tilde{I}_j(\boldsymbol{\alpha}, \boldsymbol{\gamma})] = 2\text{Re} \left[ \sum_{\tau=0}^{n-1} \tilde{c}_{\boldsymbol{\alpha}}(\tau) \exp(-i\omega_j \tau) \right] - \tilde{c}_{\boldsymbol{\alpha}}(0), \quad (15)$$

where  $\tilde{c}_{\boldsymbol{\alpha}}(\tau)$  is the expectation of the biased sample autocovariance of the modulated process, given by

$$\tilde{c}_{\boldsymbol{\alpha}}(\tau) = c_{\boldsymbol{\alpha}}(\tau) \frac{1}{n} \sum_{t=0}^{n-\tau-1} g_t g_{t+\tau}. \quad (16)$$

Then, our final debiased Whittle likelihood for mixed models which accounts for missing data is given by the following formula:

$$l_W(\boldsymbol{\alpha}, \boldsymbol{\beta}, \boldsymbol{\gamma}) = - \sum_{j=1}^n \left[ \log \tilde{f}_{\boldsymbol{\alpha}}(\omega_j) + \frac{\tilde{I}_j(\boldsymbol{\beta}, \boldsymbol{\gamma})}{\tilde{f}_{\boldsymbol{\alpha}}(\omega_j)} \right]. \quad (17)$$

This form of the Whittle likelihood retains the original computational complexity of  $O(n \log n)$  thus offering a substantial computational speed-up relative to maximum likelihood.

## 3.2 Alternative estimation methods

### 3.2.1 Gaussian maximum likelihood

Maximum likelihood estimation is a common tool across various fields of statistics due to its estimates' desirable properties, such as consistency and efficiency. The method consists in maximising the likelihood function (or optimising its appropriate transform). For the mixed model, the Gaussian likelihood function is derived from the properties of  $\epsilon(t; \boldsymbol{\alpha})$  assumed to be a Gaussian process with covariance function  $c_{\boldsymbol{\alpha}}(\tau)$ . The Gaussian log-likelihood, which is the generalisation of (8) for a mixed model, is given by

$$l(\boldsymbol{\alpha}, \boldsymbol{\beta}, \boldsymbol{\gamma}) = \text{constant} - \frac{1}{2} \log |C(\boldsymbol{\alpha})| - \frac{1}{2} (\mathbf{x} - M_{\boldsymbol{\gamma}} \boldsymbol{\beta})^T C(\boldsymbol{\alpha})^{-1} (\mathbf{x} - M_{\boldsymbol{\gamma}} \boldsymbol{\beta}), \quad (18)$$

and can be maximised to estimate the parameters  $\boldsymbol{\alpha}$ ,  $\boldsymbol{\beta}$ , and  $\boldsymbol{\gamma}$  simultaneously

As in general there is no closed-form solution to the optimisation of the likelihood function, it instead must be optimised numerically. Marchant et al. [2022] show, however, that conditional on  $\boldsymbol{\alpha}$  and  $\boldsymbol{\gamma}$ , the

function is optimised when

$$\boldsymbol{\beta} = (M_\gamma^T C(\boldsymbol{\alpha})^{-1} M_\gamma)^{-1} M_\gamma^T C(\boldsymbol{\alpha})^{-1} \mathbf{x}. \quad (19)$$

Due to this, we only need to numerically explore the space of parameters  $\boldsymbol{\alpha}$  and  $\gamma$  to find the estimates, and then obtain  $\hat{\boldsymbol{\beta}}$  analytically given the estimates  $\hat{\boldsymbol{\alpha}}$  and  $\hat{\gamma}$ . This speeds up the optimisation, but Marchant et al. [2022] note that the estimation may still be computationally expensive for large datasets due to the computational complexity of matrix inversion  $\geq O(n^2)$ . Maximum likelihood estimation accounts for missing data: for any unobserved entry  $x_i$  of  $\mathbf{x}$ , one removes the  $i$ -th row of the design matrix  $M$ , and the  $i$ -th row and column of  $C(\boldsymbol{\alpha})$ .

### 3.2.2 Two-stage estimation with the Whittle likelihood

We follow the approach by Ivanov and Prykhod'ko [2016], who proposed a two-stage estimation procedure for models composed of a regression component and a Gaussian error. The approach combines least squares estimation for the regression parameters with Whittle estimation of the covariance parameters. Ivanov and Prykhod'ko [2016] formulated the method in terms of continuous-time processes. We present a simplified two-stage procedure for processes sampled at discrete times.

In the first stage, we obtain estimates  $\hat{\boldsymbol{\beta}}$  and  $\hat{\gamma}$  as arguments that minimise the least squares expression  $(\mathbf{x} - M_\gamma \boldsymbol{\beta})^T (\mathbf{x} - M_\gamma \boldsymbol{\beta})$ . As per standard least-squares results, conditional on  $\gamma$ , the expression is minimised by  $\boldsymbol{\beta} = \hat{\boldsymbol{\beta}} = (M_\gamma^T M_\gamma)^{-1} M_\gamma^T \mathbf{x}$ . Using this property, one only needs to optimise numerically for  $\gamma$ . We note that the least squares method coincides with maximum likelihood when the errors are i.i.d. Gaussian.

In the second step, we use model residuals  $\hat{\boldsymbol{\epsilon}} = \mathbf{x} - M_{\hat{\gamma}} \hat{\boldsymbol{\beta}}$  to obtain a Whittle estimate  $\hat{\boldsymbol{\alpha}}$  of the covariance parameters. We employ the debiasing and modulated process frameworks described in Section 3.1 to improve performance with missing data. We obtain the periodogram of the modulated residuals as

$$\tilde{I}_j = \frac{1}{n} \left| \sum_{t=1}^n g_t \hat{\epsilon}_t \exp(-i\omega_j t) \right|^2, \quad (20)$$

and its expectation is analogous to (15). We then optimise the Whittle likelihood given by (17).

The two-stage estimation may significantly reduce the computational cost of parameter estimation, especially as the Whittle likelihood, rather than maximum likelihood, is used to estimate  $\boldsymbol{\alpha}$ . Nevertheless, it comes with a theoretical disadvantage: by not estimating all parameters simultaneously one adds some simplifying assumptions that may reduce the accuracy of the estimation. In particular, the first stage of the method implicitly assumes the independence of errors terms, which we explicitly assume to be correlated. This may reduce the accuracy of the estimation of the mean particularly in areas with many missing observations. Our novel method overcomes these issues by estimating parameters jointly, as proposed in Section 3.1, and we shall contrast these approaches in our simulation study in Section 4.

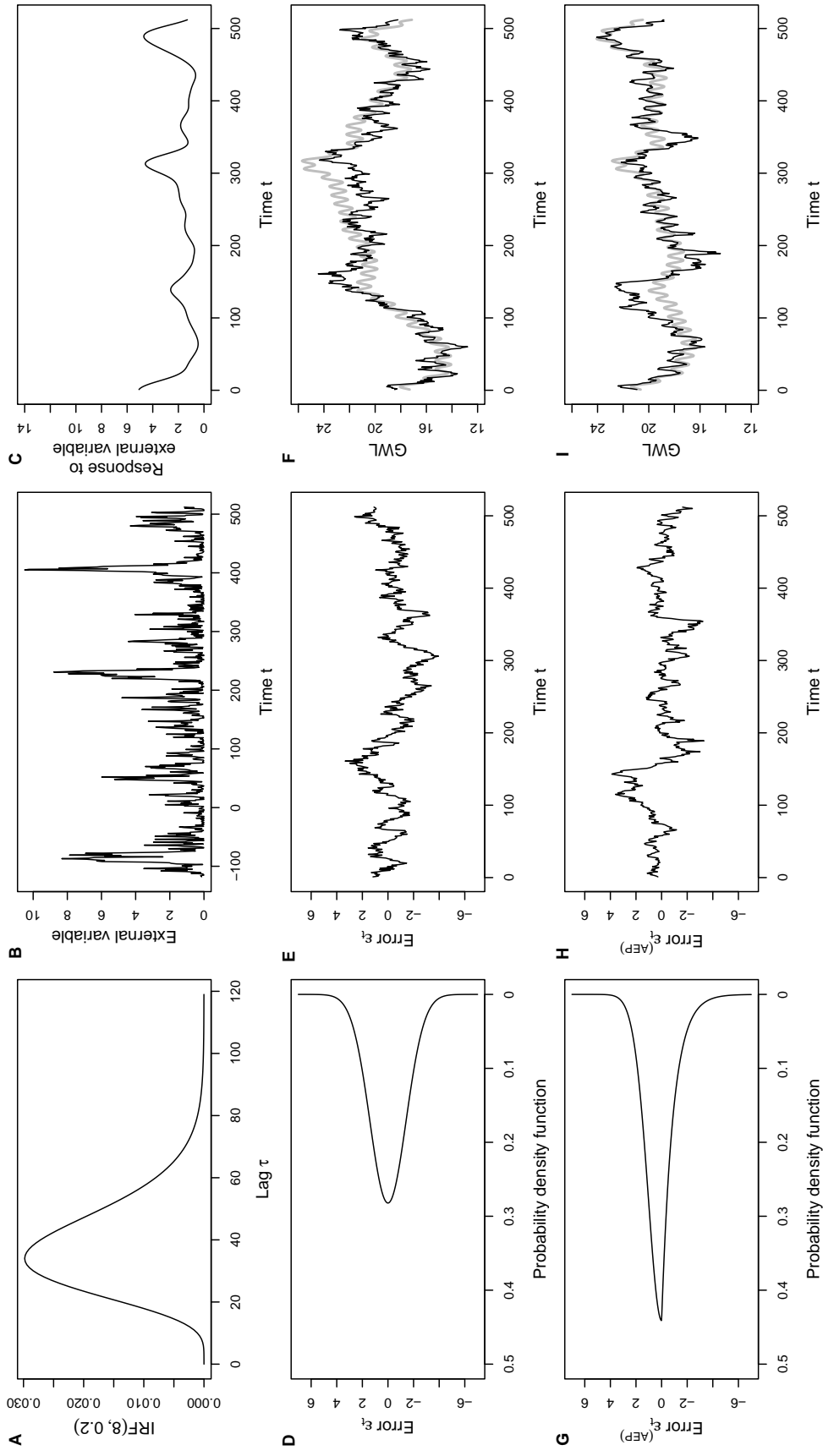
## 4 Simulation study

We conduct a simulation study to assess the performance of the three estimation methods presented in Section 3, including our novel Whittle likelihood for mixed models. We focus on aspects of the performance such as estimation and prediction errors. We consider three scenarios that reflect practical questions of interest in GWL modelling. In the first scenario, we consider the model presented in Section 2.2. Through this, we assess how well different estimation methods may perform on typical GWL data. In the second scenario we fit the same model to data generated fully randomly, i.e. with the fixed term set to zero. In this way, we assess whether the estimation method can appropriately indicate variables that are not relevant predictors of GWLs. Lastly, we consider a model with non-Gaussian errors to assess how robust the estimation methods are to model misspecification.

### 4.1 Simulation study design

For each scenario, we consider four lengths of time series  $n \in \{256, 512, 1024, 2048\}$ , where 25% of observations are missing completely at random. In all cases, we use the three estimation methods from Section 3, which we henceforth abbreviate to Whittle, maximum likelihood (ML), and 2-stage. Additionally, for the third scenario (with non-Gaussian errors), we use maximum likelihood with a correctly specified likelihood function for the non-Gaussian model from which we generate data. The main components of the data generating process in the simulation are visualised in Figure 3 with further details on each scenario as follows:

1. A **standard mixed model** is specified as the model presented in Section 2.2. Specifically, we incorporate a linear trend, seasonal variation, four cyclic splines, and a response to an external variable (e.g. rainfall). The parameter vector (in the order of these features) is  $\beta = (3, 0.15, -0.6, 18, 10, 18, 20, 1.5)^T$ . The external variable is generated by exponentiating a zero-mean Gaussian process with nested nugget Matérn covariance with parameters  $\alpha_{ext} = (0.1, 1, 15, 0.5)^T$ . We set  $n_{IRF} = 120$  and generate  $n+119$  values of the external variable. A realisation of the external variable is presented in panel B of Figure 3. The parameters controlling the IRF are  $\gamma = (8, 0.2)^T$ ; the function is plotted in panel A. In panel C, we present the GWL response to the realisation of the external variable. The error term is simulated as a Gaussian process with Matérn covariance with parameters  $\alpha = (0.05, 2, 25, 1.5)^T$ . The probability density function (pdf) of the error's marginal distribution is presented in panel D, and a realisation of the error time series is presented in panel E. Panel F combines all these components: the grey line represents the fixed term with the presented impulse response, and the black line presents a realisation of GWL time series with the presented realisation of errors. In total there are 14 parameters to be estimated across  $\{\alpha, \beta, \gamma\}$ .
2. A **fully random model** is specified by setting all entries of  $\beta$  to 0. That is, such a model consists of random errors only and panel E in Figure 3 presents a realisation of this model. We fit a standard



mixed model to the simulated data, i.e. we also estimate parameters  $\beta$  and  $\gamma$ . For the estimation, we use the same design matrix  $M_\gamma$  and external variable as in the standard mixed model scenario.

**3. A mixed model with asymmetric exponential power distribution** [AEP, Zhu and Zinde-Walsh, 2009] is specified by changing the marginal distribution of the error term. Such a model was used in the context of GWL modelling by Marchant et al. [2016] to account for potential skewness and heavy tails of the distribution of the error term. To impose a correlation structure onto the model, they used a Gaussian copula and a Matérn covariance. We follow the same approach. The AEP distribution is parameterised by five parameters: a location parameter  $\mu \in \mathbb{R}$ , a scale parameter  $\sigma > 0$ , a skewness parameter  $\varsigma \in (0, 1)$ , and left and right tail parameters  $p_1 > 0$ , and  $p_2 > 0$ , respectively. For the purpose of this paper, we set  $\mu = 0$ , but note that this does not lead to a zero-mean process, as the parameter  $\mu$  is equal to the mode, not the mean of the process [Zhu and Zinde-Walsh, 2009]. As the dispersion of the distribution is controlled by the parameter  $\sigma$ , we fix the total variance of the underlying Gaussian process to  $c_0 + c_1 = 1$  (see (5)). We simulate the AEP-distribution errors using inversion method [Nelsen, 2006, p.51], which we present step by step in Appendix A.

In this scenario, we use a simpler form of the fixed term of the mixed model to account for the greater number of parameters describing the distribution of the error term and still estimate 14 free parameters. Namely, we leave out the spline basis functions corresponding to variation in the long-term trend. Instead, we add an intercept term with parameter  $\beta_1 = 16$ . We split the unit variance of the underlying Gaussian process between the nugget  $c_0 = 0.1$  and the partial sill  $c_1 = 0.9$ . We keep the remaining parameter values the same as in the standard mixed model scenario, and additionally set  $\boldsymbol{\theta} = (\sigma, \varsigma, p_1, p_2)^T$  s.t.  $\sigma = 1.4, \varsigma = 0.4, p_1 = 1, p_2 = 1.9$ , so that the left side of the distribution has heavier tails, but, on average, only two negative errors are expected for every three positive ones. The pdf of the marginal distribution of the error is presented in panel G of Figure 3, and a realisation of the error time series is presented in panel H. Panel I combines the realisation of the error with the fixed term. As in other scenarios, we fit the mixed model assuming Gaussian errors to data generated with AEP-distributed errors. In this way, we assess how robust the methods are to model misspecification. Additionally, we use a correct log-likelihood function which does account for the AEP-distributed errors, and which we present in Appendix A.

In Table 1, we present the metrics we use to compare the performance of estimation methods in our simulation study. As the scenarios are all different, the appropriate set of metrics varies across the study, as depicted in the table and explained here in more detail. Where appropriate, we assess the accuracy of estimation of parameters  $\alpha$  and  $\beta$  using absolute proportional errors averaged for all parameters in each vector, in other words we use the  $L^1$  norm of the estimation errors divided by the true values of parameters  $\|\cdot - \cdot\|_1$  (rows 1 and 3 of Table 1). For the model with AEP-distributed errors, the parameters fitted

Table 1: Performance metrics used to compare estimation methods in three simulation scenarios.

Metric	Simulation scenario			
	Standard	Mixed	Fully Random	AEP-distributed error
$\ (\hat{\alpha} - \alpha)/\alpha\ _1$	✓		✓	✗
$\text{Div}[c_{\hat{\alpha}}(\cdot)]$	✗		✗	✓
$\ (\hat{\beta} - \beta)/\beta\ _1$	✓		✗	✓
$\ (\hat{\beta} - \beta)\ _1$	✗		✓	✗
$\text{Div}[IRF(\cdot; \hat{s}, \hat{a})]$	✓		✗	✓
RMSE( $\hat{\mathbf{x}}_{miss}$ )	✓		✓	✓

with the assumption of Gaussianity cannot be compared meaningfully with the true values. Instead, we consider a metric of divergence between the true and estimated autocovariance functions  $c_{\alpha}(\cdot)$ ,  $c_{\hat{\alpha}}(\cdot)$  of the error term:  $\text{Div}[c_{\alpha}(\cdot)] = \sum_{\tau=0}^{N-1} |c_{\alpha}(\tau) - c_{\hat{\alpha}}(\tau)|$  (row 2 of Table 1). For the fully random scenario in which  $\beta = \mathbf{0}$ , relative estimation errors cannot be computed as the truth is zero. Instead, we consider unscaled errors  $\|(\hat{\beta} - \beta)\|_1$  (row 4 of Table 1). For mixed models, we do not compare parameter estimates for  $\gamma$  directly, as they are not of immediate interest. Rather, we compare the divergence metrics between the estimated and true IRFs:  $\text{Div}[IRF(\cdot; \hat{s}, \hat{a})] = \sum_{\tau=0}^{n_{IRF}-1} |IRF(\tau; \hat{s}, \hat{a}) - IRF(\tau; s, a)|$  (row 5 of Table 1). We compare the accuracy of filling in missing values using the root mean squared error (RMSE) for all missing observations  $\mathbf{x}_{miss}$  (row 6 of Table 1), which are predicted using simple Kriging. In the scenario with AEP-distributed errors, simple Kriging is applied to model residuals converted to the Gaussian distribution (see Appendix A). Then, using the inversion method, the predicted values are converted back to the AEP distribution and added to the estimated fixed term. For all metrics, lower values indicate better performance.

## 4.2 Simulation study results

Performance metrics from the simulation study are presented in Figures 4–6, each figure showing metrics for one simulation study scenario. The results are presented as boxplots, where each datapoint represents a performance metric from one simulation run. The whiskers of boxplots represent the minimum and the 90th percentile of the recorded metric values. The highest 10% of the values are represented as dots. In cases where most extreme metric values would have compromised the legibility of the other elements of the boxplots, we cut the highest values off and report the number of points that are not displayed. Below we discuss the results by comparing the performance of different estimation methods across the three scenarios.

As expected, the correctly specified **maximum likelihood**, i.e. with Gaussian errors in the scenarios with standard mixed model and fully random model, and with AEP-distributed errors in the remaining scenario, outperformed other methods across all metrics in nearly all cases. Few exceptions from this occurred only for cases with low numbers of observations, e.g. for the IRF divergence in the standard

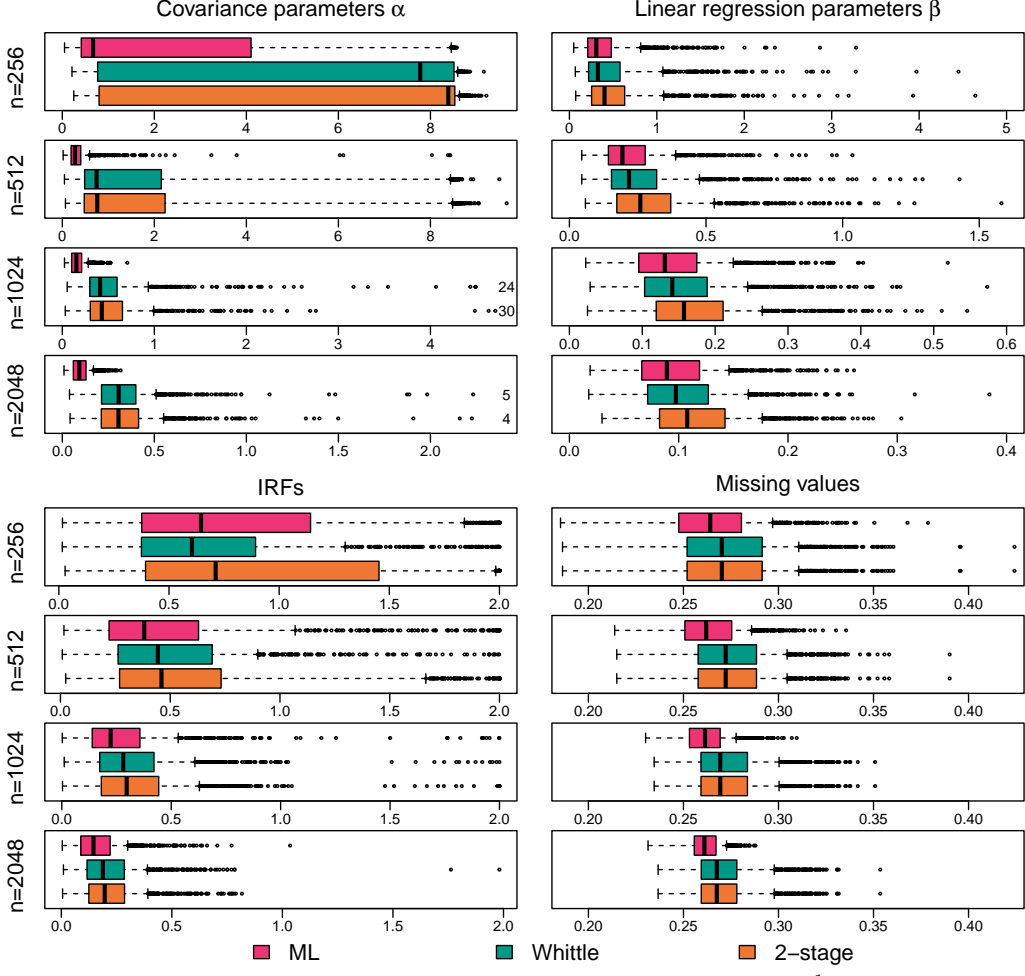


Figure 4: Simulation results for the standard mixed model scenario: boxplots of  $L^1$  relative errors of covariance parameter estimates  $\hat{\alpha}$  and linear regression parameter estimates  $\hat{\beta}$ , divergence between true and estimated IRFs, and RMSE of prediction of missing values.

mixed model scenario (Figure 4). The advantage of maximum likelihood was generally greater for the metrics related to the random error than to the fixed term of the mixed model. The advantage was smallest for the RMSE of the missing value prediction. At the same time, the advantage was overall greater in the scenario with AEP-distributed errors. Here, missing values prediction was an exception, as all methods performed similarly well.

In the scenario with AEP-distributed errors (Figure 6), maximum likelihood specified for Gaussian errors performed worse than Whittle and 2-stage. This disadvantage is visible in terms of metrics related to autocovariance of the random error, regression parameters  $\beta$ , as well as IRFs. This demonstrates that Whittle and 2-stage were more robust to non-Gaussianity than using the (misspecified) Gaussian maximum likelihood in this study. Despite this, the Gaussian maximum likelihood did not perform worse than Whittle and 2-stage when it came to missing value prediction, as also shown by Marchant et al. [2016].

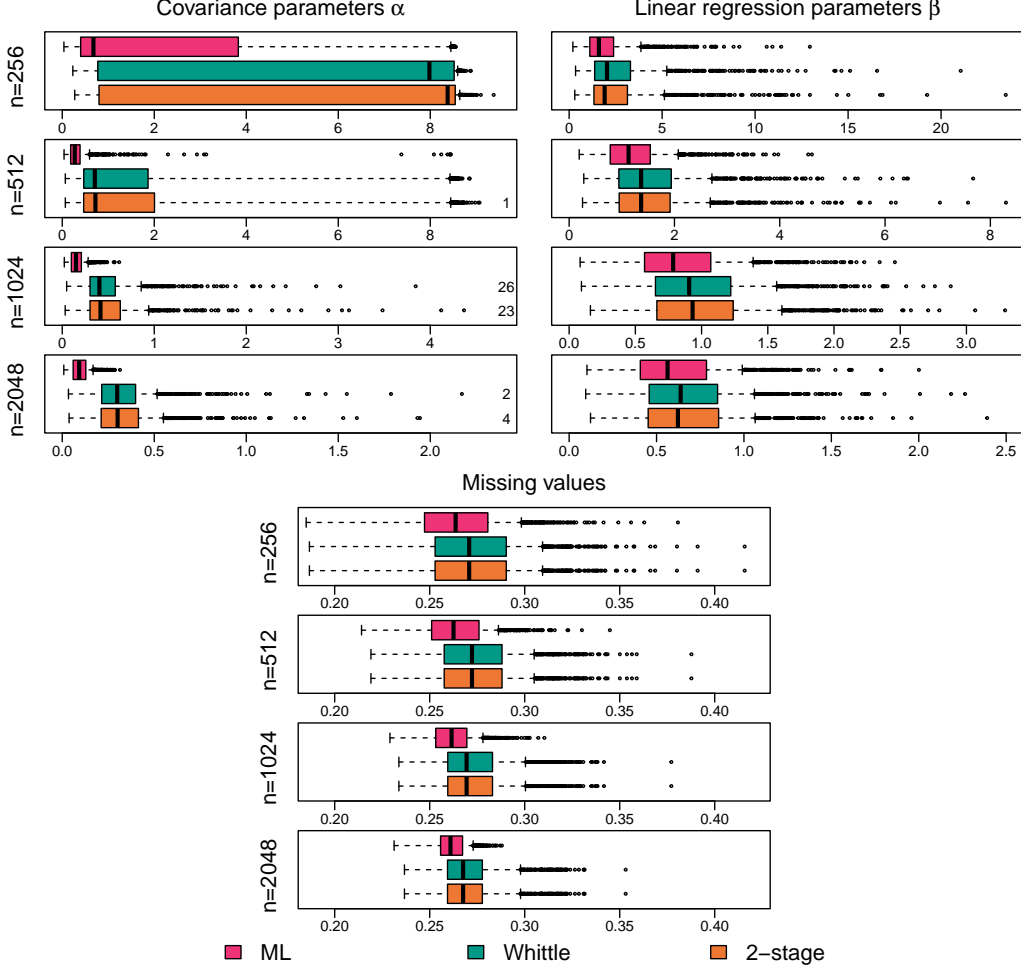


Figure 5: Simulation results for the fully random model scenario: as in Figure 4 except with absolute (instead of relative)  $L^1$  errors of covariance estimates  $\hat{\beta}$  and without metrics for IRF divergence.

**Whittle** and **2-stage** performed similarly well at predicting missing values in each scenario. The advantage of Whittle over 2-stage is most visible in the standard mixed model scenario (Figure 4), which represents a typical case of GWL data. Here, Whittle slightly outperformed 2-stage at the estimation of covariance parameters  $\alpha$ , and more substantially of the regression parameters  $\beta$ . In the latter case, the performance metrics of Whittle were closer to maximum likelihood than to 2-stage. When it comes to divergence of true and estimated IRFs, the advantage of Whittle was larger for shorter time-series and diminished with increasing  $n$ . In the fully random model scenario (Figure 5), there was a slight advantage of Whittle over 2-stage in terms of the estimation of covariance parameters  $\alpha$ . Unlike in the standard mixed model scenario, here both methods performed similarly well when regression parameters  $\beta$  were concerned, meaning that the two methods had a similar ability to discern insignificant predictors of the fixed term of the mixed model. In the scenario with AEP-distributed errors (Figure 6), the performance metrics for Whittle had better central percentiles (25th, 50th, 75th) than 2-stage when one considers the estimation of linear regression parameters  $\beta$  or IRFs (except when  $n = 512$ ). At the same time, the

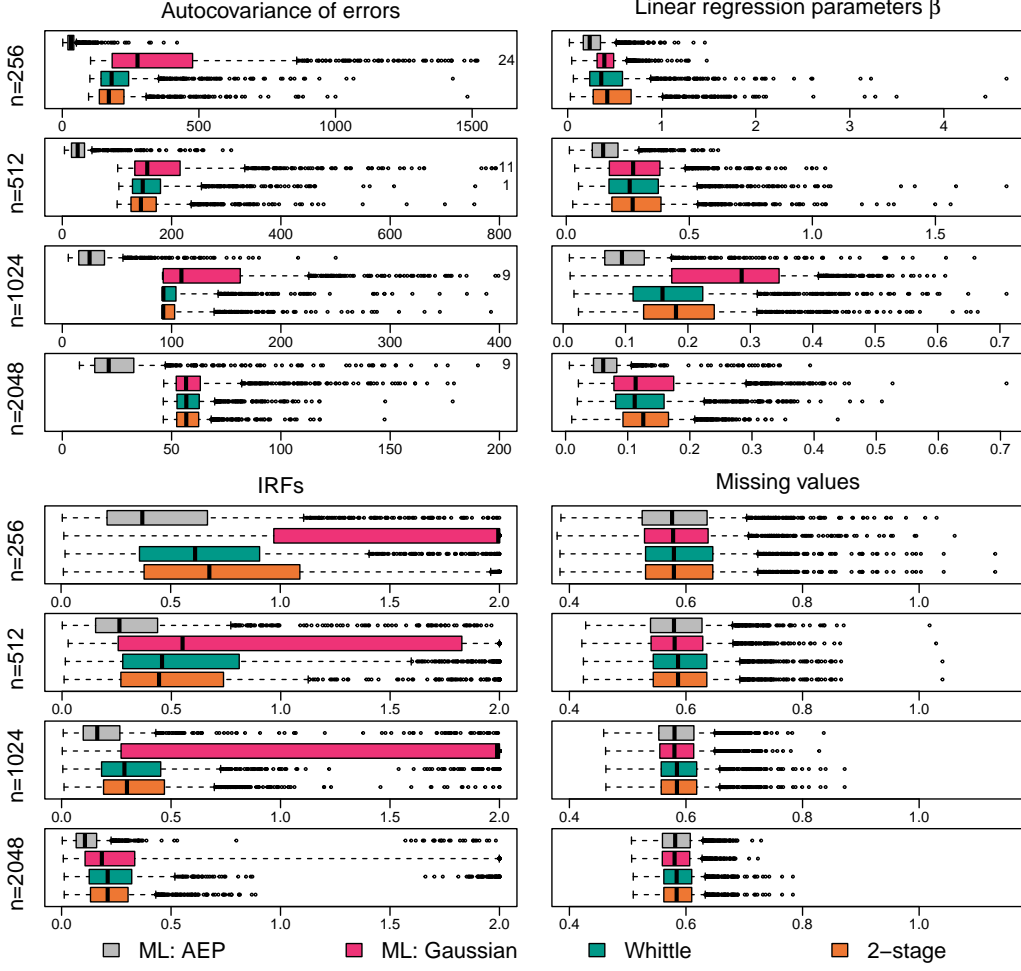


Figure 6: Simulation results for the AEP-distributed errors scenario: as in Figure 4 except with divergence between true and estimated autocovariance of random errors instead of estimation errors of covariance parameters.

tails of the distributions of the metrics were a bit heavier for Whittle. In terms of the remaining metrics, both methods resulted in a similar performance. For the shorter time series, Whittle exhibited a slight disadvantage in terms of divergence of true and estimated autocovariance of random errors.

The results of the study demonstrated that Whittle can be successfully applied to typical GWL data with missing values. It offered an improvement over 2-stage while being more computationally efficient than maximum likelihood. For AEP-distributed errors, the two Whittle-based methods were more robust to non-Gaussianity than using a misspecified maximum likelihood assuming Gaussian errors.

## 5 Application

We now fit the mixed model to the GWL time series presented in Section 2.1. We compare two estimation methods: Whittle, which we use to estimate models with a Matérn-periodic (borehole A; with a yearly period) and Matérn (boreholes B–F) covariance, as well as Gaussian maximum likelihood, which we use

to estimate models with exponential covariance. By using a simpler covariance function with maximum likelihood we follow the modelling approach by Marchant and Bloomfield [2018] and Marchant et al. [2022], which reflects the standard practice, and we ensure the comparison between maximum likelihood and Whittle is fairer in terms of required computation time. We note that maximum likelihood still required, on average, computation time longer by 30.38% than Whittle for time series of length 720. Due to the different computational complexities of maximum likelihood ( $O(n^3)$ ) and Whittle ( $O(n \log n)$ ), the difference would be much larger for longer GWL time series contained in the Environment Agency's Hydrology Explorer. We find, as expected given the results of our simulation study, that maximum likelihood and Whittle lead to very similar mean (fixed term) estimates and missing value predictions. We present the estimates and predictions obtained using Whittle in Figure 2.

We now assess key model diagnostics of the error term. Figure 7 presents the empirical autocovariance of model residuals and autocovariance functions with estimated parameters. The covariance functions estimated using both maximum likelihood and Whittle were similar to the empirical ones for borehole C, and to a lesser extent for boreholes B and E, suggesting that for these boreholes the exponential covariance provided a relatively good fit to the data. For boreholes A, D, and F, there were substantial gaps between the empirical covariance and exponential covariance, suggesting that this covariance model was not flexible enough to describe the behaviour of the random error. Such gaps were lessened for boreholes D and F when a Matérn covariance was estimated using Whittle. For borehole A, a good fit was achieved after estimating (using Whittle) a model with Matérn-periodic covariance.

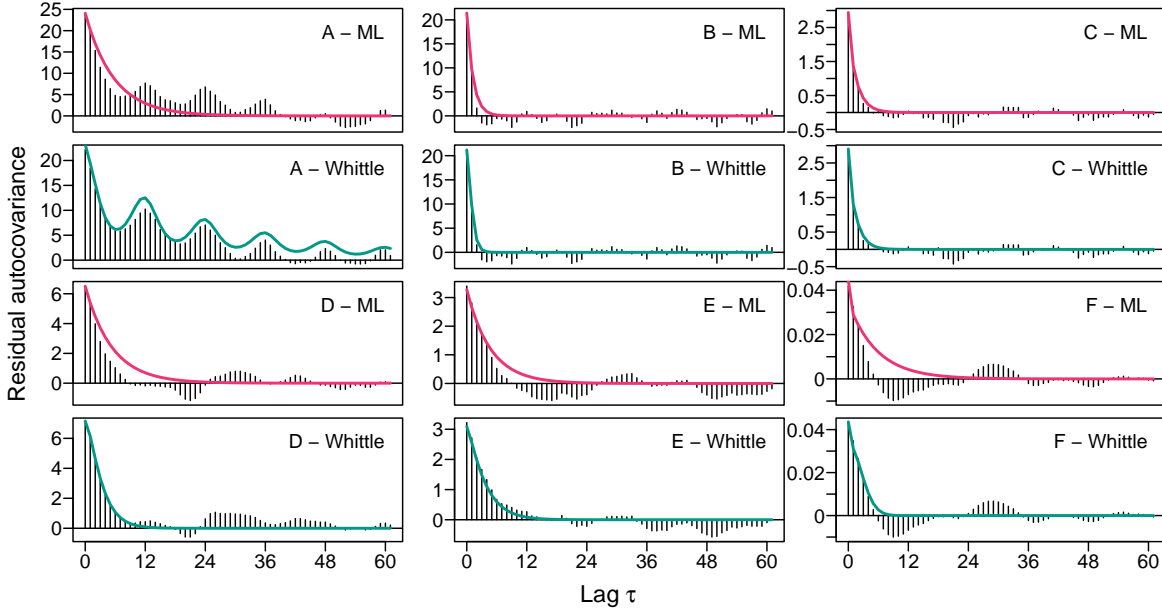


Figure 7: Empirical autocovariance of model residuals (bars) and covariance functions using parameter estimates obtained using maximum likelihood (magenta, exponential covariance) and Whittle (teal, Matérn and Matérn-periodic covariance) for boreholes A-F.

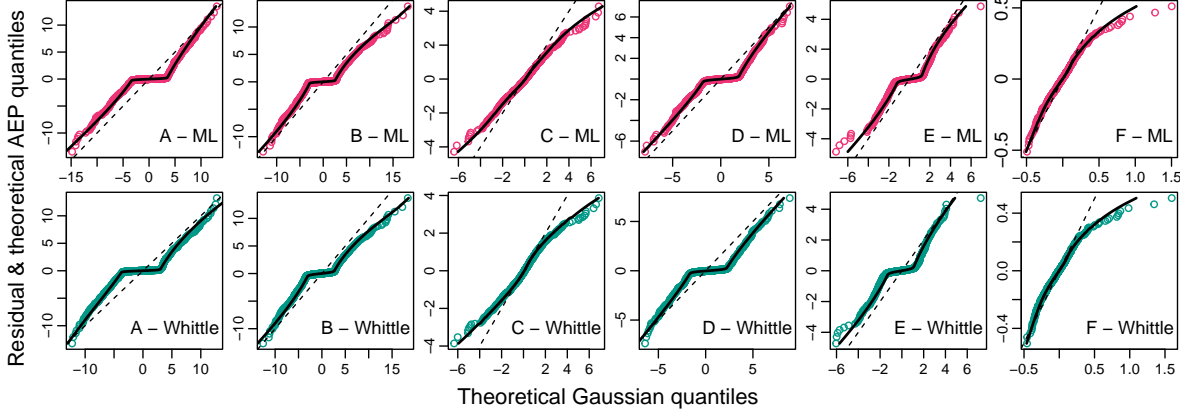


Figure 8: Q-Q plots of quantiles of residuals from mixed models estimated using maximum likelihood and Whittle (magenta and teal circles, respectively) as well as quantiles of AEP distributions fitted to the residuals (solid lines) against quantiles of theoretical Gaussian distribution using parameter estimates from the mixed models (dashed lines) for boreholes A–F.

Figure 8 presents Q-Q plots of model residuals against theoretical Gaussian quantiles. Clear departures from Gaussianity can be seen in all figures regardless of inference method used. This suggests that random errors were not Gaussian, which invalidates a key assumption of Gaussian maximum likelihood. The figure also juxtaposes the distributions of model residuals with AEP distributions fitted to the residuals. Using AEP improved the fit in all cases, although some minor departures in the tails of the distributions were still present (see E–F). This suggests that for the presented data, the AEP distribution was a more appropriate model for the random error than a Gaussian distribution. We note that the full 17-parameter mixed model (including spline basis functions) with AEP-distributed errors required much longer computation time than Whittle and Gaussian maximum likelihood, and optimisation algorithms converged to local minima.

Finally, we assessed the predictive power of the fitted models. We randomly removed and predicted (using Kriging) 12 monthly values using gaps of either: 12( $\times 1$ ), 6( $\times 2$ ), or 3( $\times 4$ ) months of consecutively missing data. In each case the introduced gaps neighboured observed values. We repeated the procedure 250 times. Table 2 shows how using Whittle reduced the RMSE of predictions relative to Gaussian maximum likelihood. Whittle offered the greatest improvement for boreholes A and F, for which the model fit differed the most between Whittle and ML (see Figure 7). For borehole A, the yearly periodicity in the covariance of the model residuals corresponded to an especially large improvement for the 12-month gaps. Smaller improvements were also recorded for gaps of 3 and 6 months for boreholes B and D. For 12-month gaps for borehole D, however, the RMSE for Whittle was slightly higher than for maximum likelihood. The smallest differences of less than 1% were recorded for boreholes C, E, and for 12-month gaps for borehole B, where the two methods performed similarly overall. This is likely because for these three boreholes, the advantage of using Whittle over maximum likelihood was the smallest in terms of

Table 2: Percentage reduction of RMSE of missing value prediction for Whittle relative to Gaussian maximum likelihood for introduced gaps of different lengths. Higher values indicate stronger advantage of Whittle.

Months missing	Borehole					
	A	B	C	D	E	F
12 months $\times$ 1	20.37%	0.92%	0.49%	-1.15%	0.53%	7.39%
6 months $\times$ 2	15.13%	1.26%	0.67%	1.42%	-0.23%	8.19%
3 months $\times$ 4	6.60%	2.85%	0.19%	3.06%	-0.92%	9.01%

model fit to the data (see Figure 7).

## 6 Concluding remarks

This paper proposed a new Whittle-based procedure for the simultaneous estimation of mixed model parameters in time series with missing data. In a simulation study, we demonstrated that our proposed method offered an advantage over 2-stage estimation (fixed and random components estimated separately), leading to estimates and predictions closer to those from Gaussian maximum likelihood, which is known to have various desirable properties if the error term is indeed Gaussian. In the scenario with an AEP-distributed error term, however, we found that Whittle outperformed Gaussian maximum likelihood with improved estimates. Such robustness to non-Gaussianity was also found in Jesus and Chandler [2017] and Sykulski et al. [2019], but less so in the study of Contreras-Cristán et al. [2006], but none of these studies explicitly compared with the Gaussian maximum likelihood estimates—our paper therefore provides a concrete example of where Whittle-based inference outperformed Gaussian maximum likelihood under misspecification in a simulation study, as well as in application.

In application to GWLs, the computational time advantage of Whittle, through the use of FFTs, allowed us to estimate more complex covariance models than the exponential covariance (used in practice with maximum likelihood). This significantly improved model fit and predictions for certain time series, for which exponential covariance was insufficiently flexible. For boreholes for which the exponential covariance already provided a good fit, Whittle still led to similar predictions as maximum likelihood in less computational time. This is in agreement with the results of our simulation study, in which we estimated equally flexible models using both Whittle and maximum likelihood, and did not observe very large differences in their predictive ability when the maximum likelihood was correctly specified.

Looking at model residuals, we found evidence of non-Gaussianity in all considered GWL time series, which violates the assumptions of Gaussian maximum likelihood. We showed that the AEP distribution fitted the residuals better. Hence, Whittle estimation should be favoured for the presented data, as it does not require a marginal distribution of error to be specified and, in our simulation study, we specifically showed that it led to better estimates than Gaussian maximum likelihood when the errors were AEP-distributed. Investigating whether such robustness to non-Gaussianity offered by Whittle

methods extends to other applications is an interesting avenue of future work.

## CRediT author contribution statement

Jakub J. Pypkowski: Conceptualisation (*lead*), Formal Analysis, Investigation, Methodology, Software, Visualisation, Writing — original draft. Adam M. Sykulski: Conceptualisation (*supporting*), Supervision, Writing — review & editing. James S. Martin: Conceptualisation (*supporting*), Supervision, Writing — review & editing. Ben P. Marchant: Conceptualisation (*supporting*), Data Curation.

## Software and code

*Upon the publication of the article, we will share our R code used for the simulation study and the real data analysis on GitHub.*

## Acknowledgments

This work was supported by the Department of Mathematics, Imperial College London, via a Roth Scholarship.

## A Mixed model with AEP-distributed errors: properties, simulation, and likelihood function

We first present key properties of the AEP distribution derived by Zhu and Zinde-Walsh [2009]. Let  $Z$  be an AEP-distributed random variable, and let  $z$  be its realisation. The pdf is given as

$$f(z) = \begin{cases} \frac{\varsigma}{\varsigma^* \sigma} K_{EP}(p_1) \exp\left(-\frac{1}{p_1} \left|\frac{z-\mu}{2\varsigma^* \sigma}\right|^{p_1}\right) & \text{if } z \leq \mu, \\ \frac{1-\varsigma}{(1-\varsigma^*) \sigma} K_{EP}(p_2) \exp\left(-\frac{1}{p_2} \left|\frac{z-\mu}{2(1-\varsigma^*) \sigma}\right|^{p_2}\right) & \text{if } z > \mu, \end{cases} \quad (21)$$

where  $K_{EP}(p) = [2p^{1/p}\Gamma(1+1/p)]^{-1}$  is a normalising constant, and  $\varsigma^* = \varsigma K_{EP}(p_1)/[\varsigma K_{EP}(p_1) + (1-\varsigma)K_{EP}(p_2)]$ . The cumulative distribution function (cdf) is given as

$$F(z) = \begin{cases} \varsigma \left[1 - G\left(\frac{1}{p_1} \left|\frac{z-\mu}{2\varsigma^* \sigma}\right|^{p_1}, \frac{1}{p_1}\right)\right] & \text{if } z \leq \mu, \\ \varsigma + (1-\varsigma)G\left(\frac{1}{p_2} \left|\frac{z-\mu}{2(1-\varsigma^*) \sigma}\right|^{p_2}, \frac{1}{p_2}\right) & \text{if } z > \mu, \end{cases} \quad (22)$$

where  $G(x; \lambda)$  is the one-parameter Gamma cdf. Lastly, the quantile function is given as

$$F^{-1}(\pi) = \begin{cases} \mu - 2\sigma\varsigma^* \left[ p_1 G^{-1} \left( 1 - \frac{\pi}{\varsigma}, \frac{1}{p_1} \right) \right]^{1/p_1} & \text{if } \pi \leq \varsigma, \\ \mu + 2\sigma(1 - \varsigma^*) \left[ p_2 G^{-1} \left( 1 - \frac{1-\pi}{1-\varsigma}, \frac{1}{p_2} \right) \right]^{1/p_2} & \text{if } \pi > \varsigma, \end{cases} \quad \pi \in [0, 1]. \quad (23)$$

Following Zhu and Zinde-Walsh [2009], we note that the AEP distribution has finite fourth-order moments.

To simulate AEP-distributed errors, we generate Gaussian errors with the Matérn covariance function  $c_{\alpha}(\tau)$  and convert them to AEP-distributed errors using the inversion method as described below [Nelsen, 2006, p.51]. We omit details of theory on copulas, and refer an interested reader to Nelsen [2006]. Let  $\Phi(x)$  denote the standard normal cdf. The AEP-distributed errors are then obtained as follows.

1. Generate  $\boldsymbol{\epsilon} = (\epsilon_1, \dots, \epsilon_n)$  from the zero-mean Gaussian process with Matérn covariance  $c_{\alpha}(\tau)$ .
2. Convert  $\boldsymbol{\epsilon}$  to the uniform distribution on  $(0, 1)$  as  $\boldsymbol{\epsilon}^{(U)} = (\epsilon_1^{(U)}, \dots, \epsilon_n^{(U)}) = (\Phi(\epsilon_1), \dots, \Phi(\epsilon_n))$ .
3. Convert  $\boldsymbol{\epsilon}^{(U)}$  to the AEP distribution as  $\boldsymbol{\epsilon}^{(AEP)} = (\epsilon_1^{(AEP)}, \dots, \epsilon_n^{(AEP)}) = (F^{-1}(\epsilon_1^{(U)}), \dots, F^{-1}(\epsilon_n^{(U)}))$

using the quantile function of the desired AEP distribution given in (23).

The likelihood function for a mixed model with AEP-distributed errors is specified as follows [Kazianka and Pilz, 2010; Marchant et al., 2016].

$$l_{AEP}(\boldsymbol{\alpha}, \boldsymbol{\beta}, \boldsymbol{\gamma}, \boldsymbol{\theta}) = -\frac{1}{2} \log|C(\boldsymbol{\alpha})| + \frac{1}{2} \mathbf{a}_{\boldsymbol{\theta}}^T (I_n - C(\boldsymbol{\alpha})^{-1}) \mathbf{a}_{\boldsymbol{\theta}} + \sum_{t=1}^n \log f[x_t - M_{\boldsymbol{\gamma}}^{(t)} \boldsymbol{\beta}], \quad (24)$$

where  $\mathbf{a}_{\boldsymbol{\theta}} = (a_{\boldsymbol{\theta},1}, \dots, a_{\boldsymbol{\theta},n})$  is obtained from errors  $\boldsymbol{\epsilon}^{(AEP)} = \mathbf{x} - M_{\boldsymbol{\gamma}} \boldsymbol{\beta}$  by reverting the inversion method, that is  $a_{\boldsymbol{\theta},t} = \Phi^{-1}\{F[x_t - M_{\boldsymbol{\gamma}}^{(t)} \boldsymbol{\beta}]\}$ .

## References

S. Aigrain and D. Foreman-Mackey. Gaussian process regression for astronomical time series. *Annual Review of Astronomy and Astrophysics*, 61(1):329–371, 2023. doi: <https://doi.org/10.1146/annurev-astro-052920-103508>.

J. Alman and V. V. Williams. A refined laser method and faster matrix multiplication. *TheoretCS*, 3, 2024. doi: <https://doi.org/10.1137/1.9781611976465.32>.

B. H. Baltagi, G. Bresson, and J.-M. Etienne. *Estimation of Serially Correlated Error Components Models Using Whittle’s Approximate Maximum Likelihood Method*, pages 337–365. Springer Nature Switzerland, Cham, 2025. doi: [https://doi.org/10.1007/978-3-031-92699-0\\\_12](https://doi.org/10.1007/978-3-031-92699-0\_12).

M. Bertolacci, O. Rosen, E. Cripps, and S. Cripps. Adaptspec-x: Covariate-dependent spectral modeling

of multiple nonstationary time series. *Journal of Computational and Graphical Statistics*, 31(2):436–454, 2022. doi: <https://doi.org/10.1080/10618600.2021.2000870>.

J. P. Bloomfield and B. P. Marchant. Analysis of groundwater drought building on the standardised precipitation index approach. *Hydrology and Earth System Sciences*, 17(12):4769–4787, 2013. doi: <https://doi.org/10.5194/hess-17-4769-2013>.

A. Contreras-Cristán, E. Gutiérrez-Peña, and S. G. Walker. A note on whittle’s likelihood. *Communications in Statistics-Simulation and Computation*, 35(4):857–875, 2006. doi: <https://doi.org/10.1080/03610910600880203>.

E. R. Coutinho, J. G. F. Madeira, R. M. da Silva, E. M. de Oliveira, and A. R. S. Delgado. Application of a computational hybrid model to estimate and filling gaps for meteorological time series. *Revista Brasileira de Meteorologia*, 38:1, 2023. doi: <https://doi.org/10.1590/0102-778638220030>.

R. Dahlhaus. Small sample effects in time series analysis: a new asymptotic theory and a new estimate. *The Annals of Statistics*, pages 808–841, 1988. doi: <https://doi.org/10.1214/aos/1176350838>.

R. Dahlhaus. A likelihood approximation for locally stationary processes. *The Annals of Statistics*, 28(6):1762–1794, 2000. doi: <https://doi.org/10.1214/aos/1015957480>.

K. ElHaj and D. Alshamsi. Geotemporal clustering for aquifer delineation: a big data approach to synchronizing and analyzing variable-length groundwater time series. *Journal of Big Data*, 12(1):25, 2025. doi: <https://doi.org/10.1186/s40537-025-01060-6>.

H. Gholizadeh, Y. Zhang, J. Frame, X. Gu, and C. T. Green. Long short-term memory models to quantify long-term evolution of streamflow discharge and groundwater depth in alabama. *Science of The Total Environment*, 901:165884, 2023. doi: <https://doi.org/10.1016/j.scitotenv.2023.165884>.

T. Goodwin, M. Quiroz, and R. Kohn. Dynamic linear regression models for forecasting time series with semi long memory errors. arXiv:2408.09096v2 [stat.ME], 2025. doi: <https://doi.org/10.48550/arXiv.2408.09096>.

A. P. Guillaumin, A. M. Sykulski, S. C. Olhede, J. J. Early, and J. M. Lilly. Analysis of non-stationary modulated time series with applications to oceanographic surface flow measurements. *Journal of Time Series Analysis*, 38(5):668–710, 2017. doi: <https://doi.org/10.1111/jtsa.12244>.

A. P. Guillaumin, A. M. Sykulski, S. C. Olhede, and F. J. Simons. The debiased spatial whittle likelihood. *Journal of the Royal Statistical Society Series B: Statistical Methodology*, 84(4):1526–1557, 07 2022. doi: <https://doi.org/10.1111/rssb.12539>.

M. G. Hiben, A. G. Awoke, and A. A. Ashenafi. Estimation of rainfall and streamflow missing data under uncertainty for Nile basin headwaters: the case of Ghba catchments. *Journal of Applied Water Engineering and Research*, 12(2):119–133, 2024. doi: <https://doi.org/10.1080/23249676.2023.2230892>.

L. Huang, Y. Xia, and X. Qin. Estimation of semivarying coefficient time series models with ARMA errors. *The Annals of Statistics*, 44(4):1618–1660, 2016. URL <http://www.jstor.org/stable/43974727>.

A. V. Ivanov, N. N. Leonenko, and I. V. Orlovskyi. On the whittle estimator for linear random noise spectral density parameter in continuous-time nonlinear regression models. *Statistical Inference for Stochastic Processes*, 23(1):129–169, 2020. doi: <https://doi.org/10.1007/s11203-019-09206-z>.

O. V. Ivanov and V. V. Prykhod'ko. On the Whittle estimator of the parameter of spectral density of random noise in the nonlinear regression model. *Ukrainian Mathematical Journal*, 67(8):1183–1203, 2016. doi: <https://doi.org/10.1007/s11253-016-1145-1>.

J. Jesus and R. E. Chandler. Inference with the whittle likelihood: A tractable approach using estimating functions. *Journal of Time Series Analysis*, 38(2):204–224, 2017. doi: <https://doi.org/10.1111/jtsa.12225>.

H. Kazianka and J. Pilz. Copula-based geostatistical modeling of continuous and discrete data including covariates. *Stochastic Environmental Research and Risk Assessment*, 24(5):661–673, 2010. doi: <https://doi.org/10.1007/s00477-009-0353-8>.

H. L. Koul and D. Surgailis. Testing a sub-hypothesis in linear regression models with long memory covariates and errors. *Applications of Mathematics*, 53(3):235–248, 2008. doi: <https://doi.org/10.1007/s10492-008-0007-z>.

Z. Li, O. Rosen, F. Ferrarelli, and R. T. Krafty. Adaptive Bayesian spectral analysis of high-dimensional nonstationary time series. *Journal of Computational and Graphical Statistics*, 30(3):794–807, 2021. doi: <https://doi.org/10.1080/10618600.2020.1868305>.

J. Mackay, C. Jackson, and L. Wang. A lumped conceptual model to simulate groundwater level time-series. *Environmental Modelling & Software*, 61:229–245, 2014. doi: <https://doi.org/10.1016/j.envsoft.2014.06.003>.

B. Marchant and J. Bloomfield. Spatio-temporal modelling of the status of groundwater droughts. *Journal of Hydrology*, 564:397–413, 2018. doi: <https://doi.org/10.1016/j.jhydrol.2018.07.009>.

B. Marchant, J. Mackay, and J. Bloomfield. Quantifying uncertainty in predictions of groundwater levels using formal likelihood methods. *Journal of Hydrology*, 540:699–711, 2016. doi: <https://doi.org/10.1016/j.jhydrol.2016.06.014>.

B. Marchant, D. Cuba, B. Brauns, and J. Bloomfield. Temporal interpolation of groundwater level hydrographs for regional drought analysis using mixed models. *Hydrogeology Journal*, 30(6):1801–1817, 2022. doi: <https://doi.org/10.1007/s10040-022-02528-y>.

L. Myeni, M. Moeletsi, and A. Clulow. Development and validation of an operational multi-layered model for estimation of soil moisture at point-scale in South Africa. *South African Journal of Plant and Soil*, 39(1):28–40, 2022. doi: <https://doi.org/10.1080/02571862.2021.1970832>.

R. B. Nelsen. *An Introduction to Copulas*. Springer Series in Statistics. Springer New York, New York, NY, 2nd ed. 2006. edition, 2006. doi: <https://doi.org/10.1007/0-387-28678-0>.

I. Neumann, S. Brown, P. L. Smedley, and T. Besien. Baseline Report Series: 7. The Great and the Inferior Oolite of the Cotswold district. British Geological Survey Commissioned Report CR/03/202N, 2003. URL <https://nora.nerc.ac.uk/id/eprint/3572>.

D. B. Percival and A. T. Walden. *Spectral Analysis for Physical applications: Multitaper and Conventional Univariate Techniques*. Cambridge University Press, Cambridge, 1993. doi: <https://doi.org/10.1017/CBO9780511622762>.

T. Peterson and A. Western. Nonlinear time-series modeling of unconfined groundwater head. *Water Resources Research*, 50(10):8330–8355, 2014. doi: <https://doi.org/10.1002/2013WR014800>.

T. J. Peterson and A. W. Western. Statistical interpolation of groundwater hydrographs. *Water Resources Research*, 54(7):4663–4680, 2018. doi: <https://doi.org/10.1029/2017WR021838>.

S. M. Rahman, M. A. H. Babla, R. Sultana, S. Saba, and A. Hoque. Estimation of missing daily temperature and rainfall for longer durations at Hatiya and Sandwip islands in the Bay of Bengal. *Journal of Earth System Science*, 133(2):109, 2024. doi: <https://doi.org/10.1007/s12040-024-02318-y>.

O. Rosen, S. Wood, and D. S. Stoffer. AdaptSPEC: adaptive spectral estimation for nonstationary time series. *Journal of the American Statistical Association*, 107(500):1575–1589, 2012. doi: <https://doi.org/10.1080/01621459.2012.716340>.

Z. P. Shabalala, M. E. Moeletsi, M. I. Tongwane, and S. M. Mazibuko. Evaluation of infilling methods for time series of daily temperature data: Case study of Limpopo Province, South Africa. *Climate*, 7(7):86, 2019. doi: <https://doi.org/10.3390/cli7070086>.

A. M. Sykulski, S. C. Olhede, A. P. Guillaumin, J. M. Lilly, and J. J. Early. The debiased Whittle likelihood. *Biometrika*, 106(2):251–266, 02 2019. doi: <https://doi.org/10.1093/biomet/asy071>.

M. Tanguy, H. Dixon, I. Prosdocimi, D. Morris, and V. Keller. *Gridded estimates of daily and monthly areal rainfall for the United Kingdom (1890-2019) [CEH-GEAR]*. NERC EDS Environmental Information Data Centre, 2021. doi: <https://doi.org/10.5285/dbf13dd5-90cd-457a-a986-f2f9dd97e93c>.

W. F. Trench. An algorithm for the inversion of finite toeplitz matrices. *Journal of the Society for Industrial and Applied Mathematics*, 12(3):515–522, 1964. doi: <https://doi.org/10.1137/0112045>.

H. A. van Lanen, G. Laaha, D. G. Kingston, T. Gauster, M. Ionita, J. P. Vidal, R. Vlnas, L. M. Tallaksen, K. Stahl, J. Hannaford, et al. Hydrology needed to manage droughts: the 2015 European case. *Hydrological Processes*, 30(17):3097–3104, 2016. doi: <https://doi.org/10.1002/hyp.10838>.

M. N. M. van Lieshout. *Theory of spatial statistics: A concise introduction*. Chapman and Hall/CRC, 2019. doi: <https://doi.org/10.1201/9780429052866>.

J. R. von Asmuth and M. F. Bierkens. Modeling irregularly spaced residual series as a continuous stochastic process. *Water Resources Research*, 41(12), 2005. doi: <https://doi.org/10.1029/2004WR003726>.

J. R. von Asmuth, M. F. Bierkens, and K. Maas. Transfer function-noise modeling in continuous time using predefined impulse response functions. *Water Resources Research*, 38(12):23–1, 2002. doi: <https://doi.org/10.1029/2001WR001136>.

M. Vu, A. Jardani, N. Massei, and M. Fournier. Reconstruction of missing groundwater level data by using long short-term memory (LSTM) deep neural network. *Journal of Hydrology*, 597:125776, 2021. doi: <https://doi.org/10.1016/j.jhydrol.2020.125776>.

T. Wang and Y. Xia. Whittle likelihood estimation of nonlinear autoregressive models with moving average residuals. *Journal of the American Statistical Association*, 110(511):1083–1099, 2015. doi: <https://doi.org/10.1080/01621459.2014.946513>.

H. Wei, H. Zhang, H. Jiang, and L. Huang. On the semi-varying coefficient dynamic panel data model with autocorrelated errors. *Computational Statistics & Data Analysis*, 173:107458, 2022. doi: <https://doi.org/10.1016/j.csda.2022.107458>.

P. Whittle. Estimation and information in stationary time series. *Arkiv för Matematik*, 2(5):423–434, 1953. doi: <https://doi.org/10.1007/BF02590998>.

S. N. Wood. *Generalized Additive Models: an Introduction with R*. Chapman and Hall/CRC, 2017. doi: <https://doi.org/10.1201/9781315370279>.

W. Yu, Y. Liu, Z. Ma, and J. Bi. Improving satellite-based PM2.5 estimates in China using Gaussian processes modeling in a Bayesian hierarchical setting. *Scientific Reports*, 7(1):7048, 2017. doi: <https://doi.org/10.1038/s41598-017-07478-0>.

Y. Zhang and P. J. Thorburn. Handling missing data in near real-time environmental monitoring: A system and a review of selected methods. *Future Generation Computer Systems*, 128:63–72, 2022. doi: <https://doi.org/10.1016/j.future.2021.09.033>.

Y. Zhou and W. Li. A review of regional groundwater flow modeling. *Geoscience Frontiers*, 2(2):205–214, 2011. doi: <https://doi.org/10.1016/j.gsf.2011.03.003>.

D. Zhu and V. Zinde-Walsh. Properties and estimation of asymmetric exponential power distribution. *Journal of Econometrics*, 148(1):86–99, 2009. doi: <https://doi.org/10.1016/j.jeconom.2008.09.038>.